**Original Article**

# THE INFLUENCE OF ANIONS ON THE RELEASE OF AG(I) FROM SILVER NANOPARTICLES (AGNPS).

**[1]Nomor Steve Aondoakaa and [2]Horrocks Benjamin Richard**

[1]Department of Chemistry, Rev. Fr. Moses Orshio Adasu University Makurdi, Nigeria

[2]Department of Chemistry, Bedson Building, Newcastle University, Newcastle upon Tyne, NE1 7RU, UK

## ABSTRACT

*Silver nanoparticles (AgNPs) were prepared by the citrate reduction method in pure water. They were infused with and dialysed against various concentrations of chloride and sulphate salts to determine the effect of the medium on the release of Ag(I). The AgNPs were characterised by UV-Vis spectrometry, dynamic light scattering (DLS) and atomic force microscopy (AFM), while the concentration of Ag(I) ions released was monitored by anodic stripping voltammetry (ASV). The mean hydrodynamic diameters of AgNPs as measured by DLS ranged from 100 nm in the 10 mmol chloride before dialysis to 890 nm in the 50 mmol sample after dialysis. In general, the increase was due to aggregation. Individual particle sizes as measured by AFM decreased after dialysis; this suggests corrosion of the AgNPs. The release of Ag(I) as monitored by anodic stripping voltammetry at glassy carbon electrodes revealed that: (i) substantial (90 µmol) Ag(I) was present in the initial preparation and (ii) the concentration of Ag(I) after 73 h of dialysis was about 4 µmol irrespective of the concentration of chloride present. Presence of sulphates, however, did not prove to exert significant influence on the release of Ag(I) ions from a product or substrate to which they have been incorporated. The findings in this research are important in the study of the fate of AgNPs in marine environments.*

**KEYWORDS: Silver Nanoparticles, Electrolytes, Dialysis, Aggregation, Substrate**

**Open Access**

Correspondence;

Email:
ben.horrocks@ncl.ac.uk

*Corresponding Author:
snomor@bsum.edu.ng;
nomorsteve@gmail.com

***Citation**: Nomor Steve Aondoakaa and Horrocks Benjamin Richard (2026) The Influence of Anions on The Release of Ag(I) from Silver Nanoparticles (AgNPs).*

**Date of Publication:**
Vol. 9 (1), 2026

**pp 147-167**

## INTRODUCTION

Silver nanoparticles (AgNPs) have found wide applications in a variety of products such as socks (Meyer et al., 2010; Ben et al., 2008) sports wears and wound dressings (Hebeish et al., 2014; Udapudi et al., 2012; Wilkinson et al., 2011; Maneerung et al., 2008) where they serve as antibacterials and inhibit unwanted odours. Silver nanoparticles have been incorporated in such consumer products as toothpastes and washing machine detergents (Odzak et al., 2014). AgNPs are also adsorbed on the cellulose fibres of blotting paper to work as antibacterial water filters in water and waste water treatment (Dankowich & Gray, 2011; Kaegi et al., 2011; Sharma et al., 2009). When these products are washed, the silver nanoparticles leach out and disperse in the waste water where they can release silver(I) ions (Geriano, 2009). Although the only contraindication of high levels of silver in humans is argyria (WHO, 2003), it is known to be very toxic to aquatic organisms that constitute the base of a series of food chains (Sohn et al., 2015; Aghari et al., 2012).

The action of AgNPs is partially related to the release of Ag(I) ions, therefore it is important to understand the factors that control the rate and extent of release of Ag(I). Although the electrode potential of the Ag/Ag(I) half-cell is high, about +0.8 V (Bratsch, 1989), it may be very substantially reduced by the complexation of Ag(I) or the precipitation of AgX salts. This can affect the release of Ag(I) ions in two ways: by facilitating the oxidation of AgNPs by dissolved oxygen or by suppressing the Ag(I) concentration via solubility equilibria. Electroanalytical methods can determine low levels of Ag(I) in a straightforward manner, but care must be taken because the standard preparations of AgNPs may contain either excess Ag(I) reagents or traces of the reducing agent before any corrosion or release of Ag(I) from the NPs themselves. In this study a simple dialysis experiment was employed in order to resolve some of these issues. AgNPs were dialysed against a variety of electrolytes and pure water; Ag(I) was determined in the dialysate and aliquots of the sample were taken for analysis of the remaining AgNPs.

## MATERIALS AND METHODS

Silver nanoparticles were synthesized by the method of Lee & Meisel (1982), infused with and dialysed against various concentrations of chloride and sulphate salts to determine the effect of the medium on the release of Ag(I). The AgNPs were characterised by UV-Vis spectrometry, dynamic light scattering (DLS) and atomic force microscopy (AFM) while the concentration of Ag(I) ions released was monitored by anodic stripping voltammetry (ASV).

### *Preparation of Silver Nanoparticles*

The citrate reduction method by Lee & Meisel (1982) was modified and used in the preparation of silver nanoparticles. Briefly, 18 mg or 0.018 g of $AgNO_3$ was dissolved in 100 mL of nanopure water to give a 1.06 mmol solution and brought to the boil. Exactly 2 mL of 1% tri-sodium citrate dihydrate, prepared by dissolving 0.1 g of the salt in 10 mL of nanopure water was added to the boiling mixture. A greenish-yellow sol was formed about seven minutes after the addition of the sodium citrate. The citrate reduction of silver nitrate is given by equation (1).

$$2Ag^{+} + C_6H_5O_7^{3-} \rightarrow 2Ag + C_5H_4O_5^{2-} + H^{+} + CO_2 \qquad (1)$$

where $C_5H_4O_5^{2-}$ is the conjugate base of acetone dicarboxylic acid (Kuyper, 1933). The AgNPs prepared by the citrate reduction method were relatively stable as they showed neither obvious aggregation nor colour change upon standing for about three months. Pictures of freshly prepared AgNPs are shown in Figure 1.

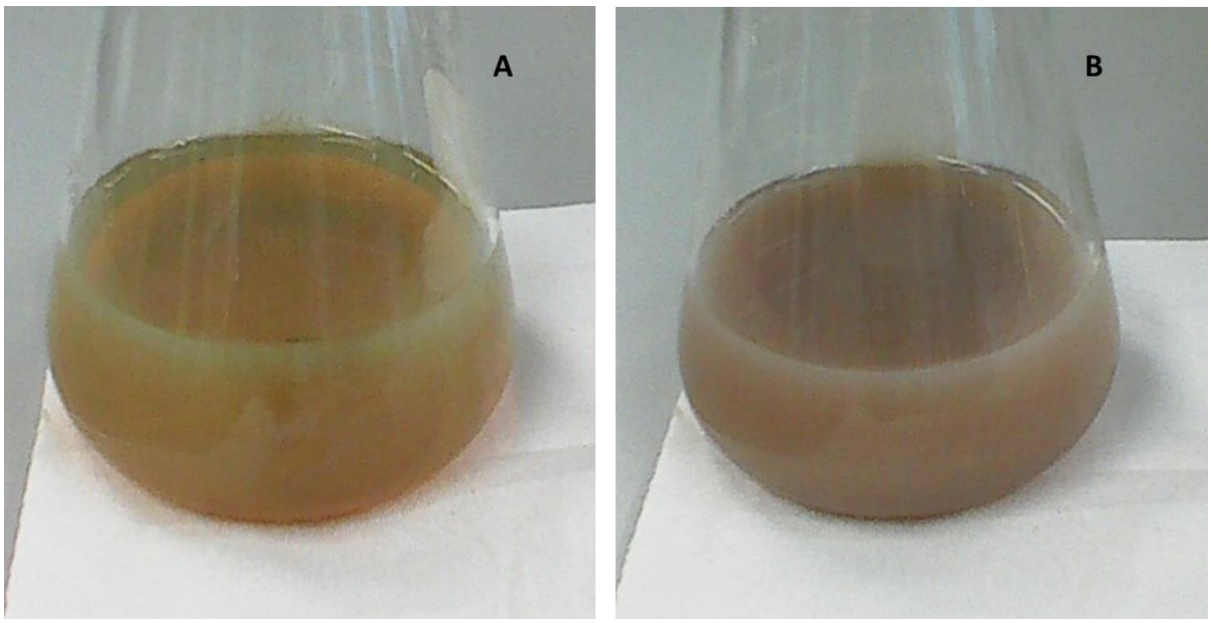



*Figure 1 Freshly prepared 10 mmol AgNPs of (A) pure water and (B) NaCl(aq) contained in 250 mL conical flasks. The NaCl(aq)-AgNPs turned turbid after addition of NaCl crystals. The NPs were prepared by the citrate reduction method*

## Characterization Techniques

### *Ultraviolet-visible (UV-Vis) spectroscopy*

Stability tests on the AgNPs were conducted via optical spectroscopy using a Cary 100 Bio UV-Vis spectrophotometer (Agilent Technologies, USA).

### *Dynamic light scattering (DLS)*

Dynamic light scattering (DLS) measurements were carried out using a Malvern high performance particle sizer (HPPS) incorporated with a non-invasive back scatter (NIBS) technology (Malvern Instruments Limited, Worcs, UK). This technology allows for high sensitivity measurement of samples as dilute as 0.1 ppm in disposable plastic or glass cuvettes while the back-scatter optics enables concentrated samples of the order of 100,000 ppm and particle size up to 10,000 nm to be measured.

### *Atomic force microscopy (AFM)*

Samples for Atomic force microscopy (AFM) imaging were prepared by drop casting 2 µL of aliquot on Si wafer that had been cleaned with acid piranha solution (3:1 solution of concentrated sulphuric acid and hydrogen peroxide), rinsed with nanopure water and dried in a stream of nitrogen gas. The drop was allowed to dry after which AFM images were obtained in the tapping mode $^{TM}$ with a Dimension Nanoscope V atomic force microscope (Veeco Inc. Metrology group Brussels, Belgium using NanoProbe tips model TAP300 AI-G of Budget Sensors USA). The cantilever was of resonant frequency 300 kHz with a force constant of 40 N/m and length of 125 µm.

### *Dialysis*

The analyte samples were contained inside dialysis membranes that were

surrounded by dialysates whose volumes were integral multiples of the volume of the samples. This arrangement was to create a concentration gradient that would allow particles to diffuse into and out of the dialysis membrane until equilibrium is established. The dialysis time was decreased by stirring and to maintain a high concentration gradient of diffusible particles across the membrane. The dialysate were changed from time to time to re-create the concentration gradient that is necessary for the efficiency of the dialysis process.

Different electrolytes were added to the as-prepared dispersions of AgNPs in order to study the effect of the anions and their concentrations on the release of Ag(I) ions from the nanoparticles. In NaCl-AgNPs, three different concentrations of aqueous NaCl; 10 mmol, 30 mmol, and 50 mmol were used.

For the 10 mmol NaCl-AgNPs, 0.0584 g of sodium chloride (molecular mass 58.44 g $mol^{-1}$) was measured and infused into 100 mL of the AgNPs while 0.5844 g/L of the NaCl(aq) solution was used as dialysate. In case of the 30 mmol concentration, 0.1753 g of the salt was infused into 100 mL of AgNPs while 1.7532 g/L of solution served as the dialysate. In a similar vein, 0.2922 g of NaCl was weighed and incorporated into 100 mL of AgNPs to give the 50 mmol NaCl-AgNPs and 2.922 g/L of the NaCl(aq) solution was prepared and used as the dialysate.

Only a 10 mmol concentration of sodium sulphate, $Na_2SO_4$ was used to monitor the effect of sulphate ion on the release of Ag(I) ions from silver nanoparticles. This is because stripping peaks for Ag(I) ions could not be obtained even at this low concentration beyond the second fraction of dialysate in spite of increasing the deposition time to 300 s. Anhydrous $Na_2SO_4$, an ACS reagent of ≥ 99% purity and molar mass 142.04 g $mol^{-1}$ was purchased from Sigma Aldrich UK. 0.142 g of the salt was weighed and incorporated into 100 mL of silver nanoparticles. The dialysate was prepared by dissolving 1.4204 g of the salt in enough of nanopure water to give a one-litre solution.

Dialysis cellulose membranes of average width diameter 35 mm, used in the purification of prepared metal nanoparticles were purchased from Sigma Aldrich, UK. The membranes with an inflated diameter of approximately 21 mm and length of 30 cm had a pore size of 12,000 Da MWCO (molecular weight cut-off). This means that the membranes could retain particles with M.W>12,000 Da.

Water used for preparation of electrolyte solutions, rinsing of electrodes and glassware as well as soaking of dialysis membranes was collected directly from the purifying source, NANOpure RO operating at a resistivity of 18.2 MΩ.cm, model DH 931 of Barnstead International, Dubuque, Iowa, USA. A picture of the apparatus used for dialysis is shown in Figure 2.

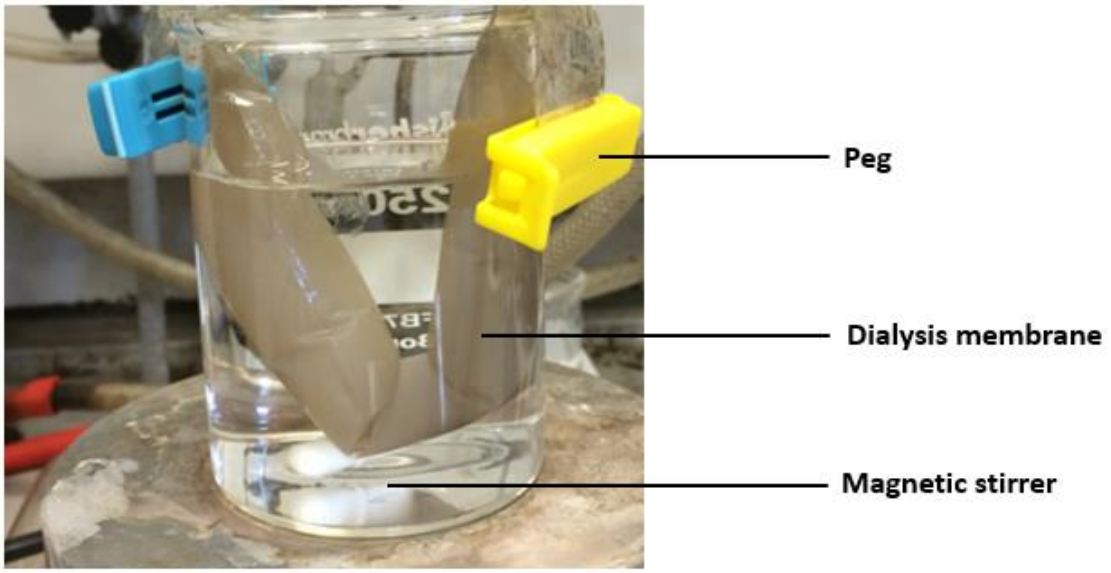
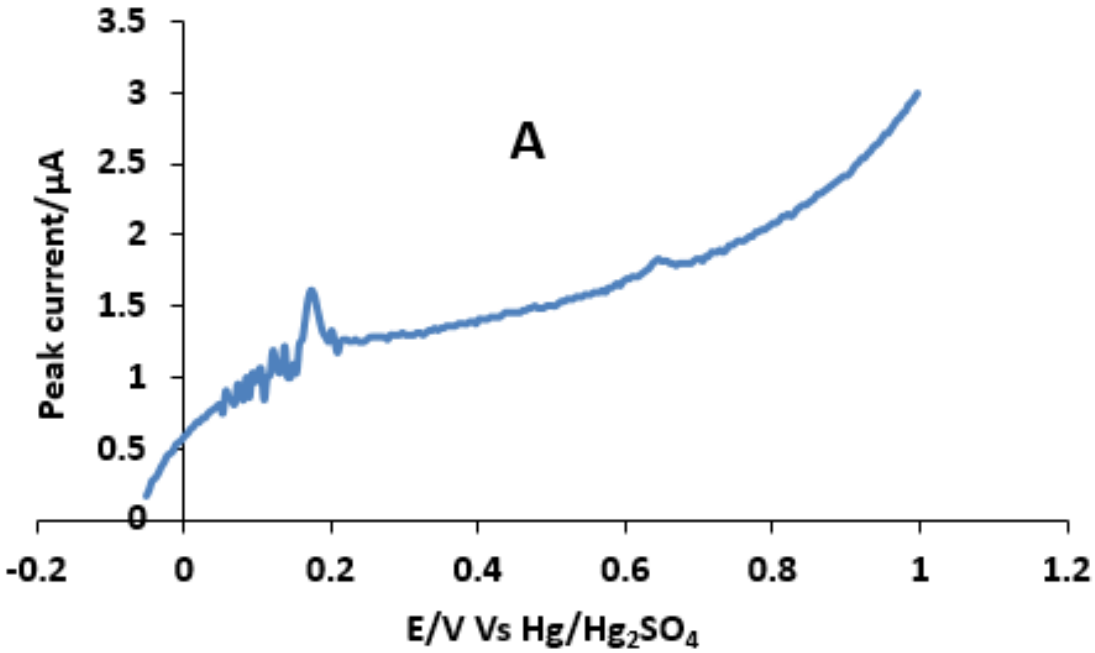



*Figure 2. Apparatus showing dialysis of 10 mmol NaCl(aq)-AgNPs contained in a 400 mL beaker*

*Anodic stripping voltammetry (ASV)*

The amount of Ag(I) ions released from the nanoparticles through the dialysis membrane was monitored by stripping voltammetry at glassy carbon, with $Hg/Hg_2SO_4$ as reference electrode for an accumulation time of 30 s. The accumulation time was increased to 300 s for dialysate fractions in which a stripping curve was not observable after 30 s of pre-concentration time. In such cases, the signal was scaled by a factor of 10 to take account of the change in deposition time. Examples of stripping curves obtained are shown in Figure 3.



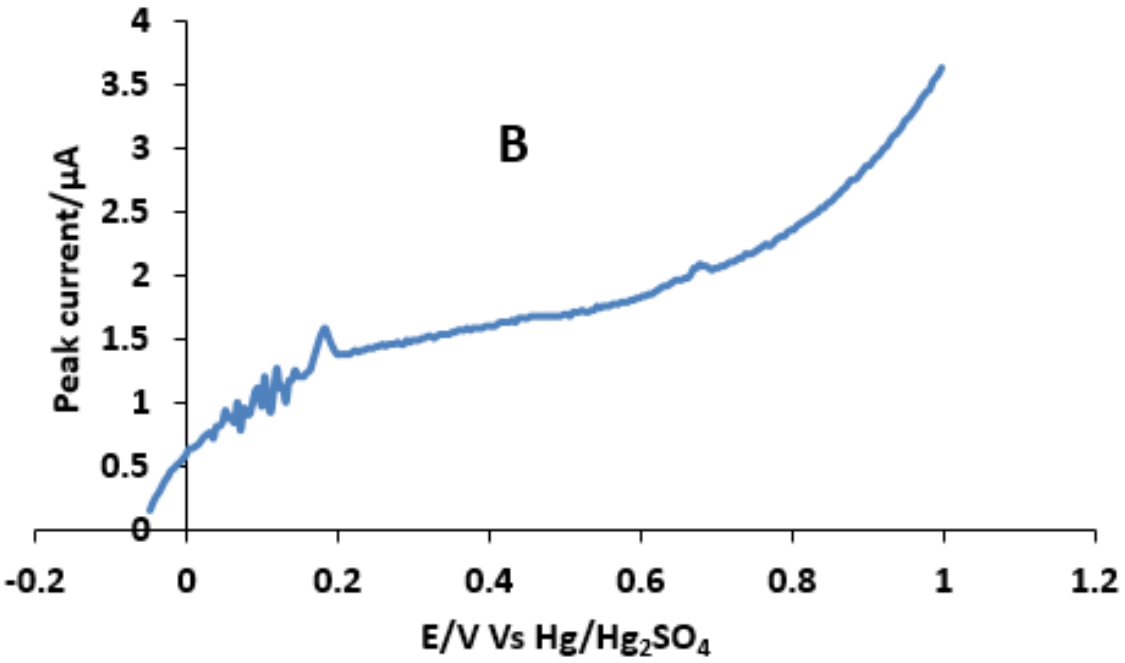



*Figure 3. (A) Anodic stripping voltammogram for 1st fraction of 50 mmol NaCl(aq)-AgNPs dialysate at glassy carbon. (B) Anodic stripping voltammogram for 5th fraction of 50 mmol NaCl(aq)-AgNPs dialysate at glassy carbon. The data is presented as was acquired, before baseline correction. The Ag stripping peaks are observed just below 0.2 V and the scan rate was 1 V $s^{-1}$.*

## RESULTS AND DISCUSSION

The surface plasmon resonance (SPR) peak of the pure water AgNP preparation was observed at 445 nm and a peak absorbance of 0.76. This spectrum is presented in Figure 4.

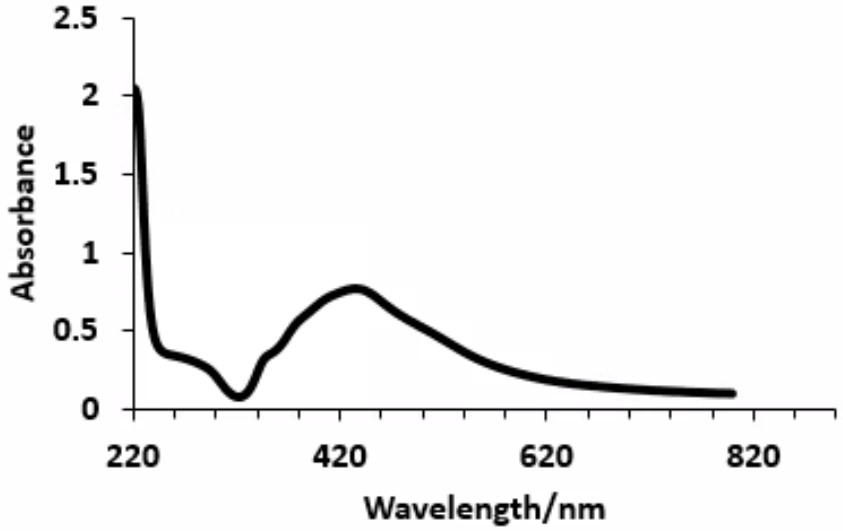



*Figure 4.UV-Vis absorption spectrum of pure water AgNPs before dialysis*

After dialysis, however, the surface plasmon peak wavelength was observed to decrease to 423 nm but the absorbance increased to 1.28 as can be observed in the spectrum of Figure 5.

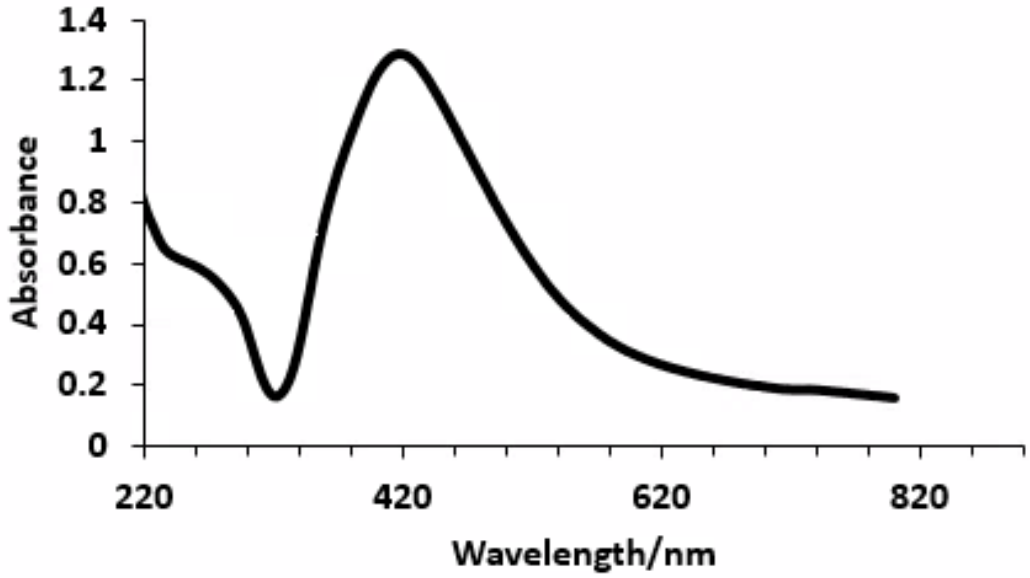



*Figure 5.UV-Vis absorption spectrum of AgNPs after dialysis against pure water for 73 h.*

This hypsochromic effect (blue-shift) can be explained on the basis of a reduction in particle size due to corrosion of the AgNPs by dissolved oxygen. In a similar manner to quantum confinement, the plasmon energy increases with decreasing size (Ghosh & Pal, 2007).

The optical absorption spectra of the sodium chloride and $Na_2SO_4$-AgNPs, however, showed a red-shift in the surface plasmon band, indicating aggregation (Hu et al., 2016; Shrivas et al., 2016; Suchomel et al., 2015; Toh et al., 2015; Odzak et al., 2014; Espinoza et al., 2012; Ijaz-Hussain et al., 2011; Khan et al., 2011; Nanda & Saravanan, 2009; Solomon et al., 2007 Wang et al., 2005) of the nanoparticles and an increase in their effective size by interparticle coupling of the plasmons. This effect that is due to the sulphate ions as shown in Figure 6.

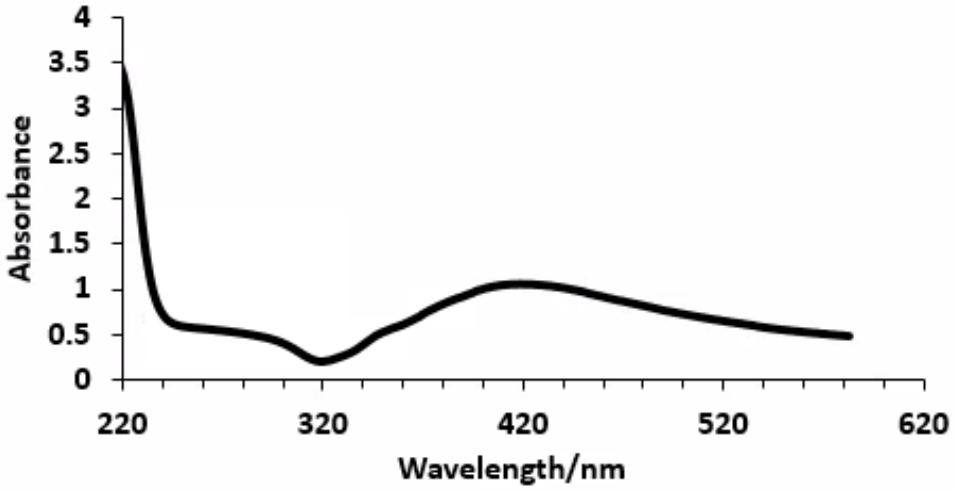



*Figure 6.UV-Vis absorption spectrum of 10 mmol $Na_2SO_4$-AgNPs before dialysis with a peak wavelength of 420 nm and a peak absorbance of 1.06*

Dynamic light scattering measures the hydrodynamic size of the particles and not directly their physical sizes. This implies that the diameter measured by this technique may include the hydration layer for pure water AgNPs or the adsorbed anions in the aqueous NaCl and $Na_2SO_4$ preparations of AgNPs as well as any ligands bound to the particle surface during the preparation. In the generated data, there is a general increase in mean sizes of nanoparticles as measured by DLS before and after dialysis. While the increase in diameter from 31.1 nm to 34.2 nm may be regarded as marginal for pure water AgNPs, the difference is pronounced in the NaCl-AgNPs, signifying the effect of the medium on the extent of aggregation. This increase of nanoparticle sizes as influenced by different media and exposure over a long period of time has been reported by other researchers (Odzak et al., 2014) in the field. The DLS analysis data of pure water AgNPs before and after dialysis are shown in Figure 7 and Figure 8.

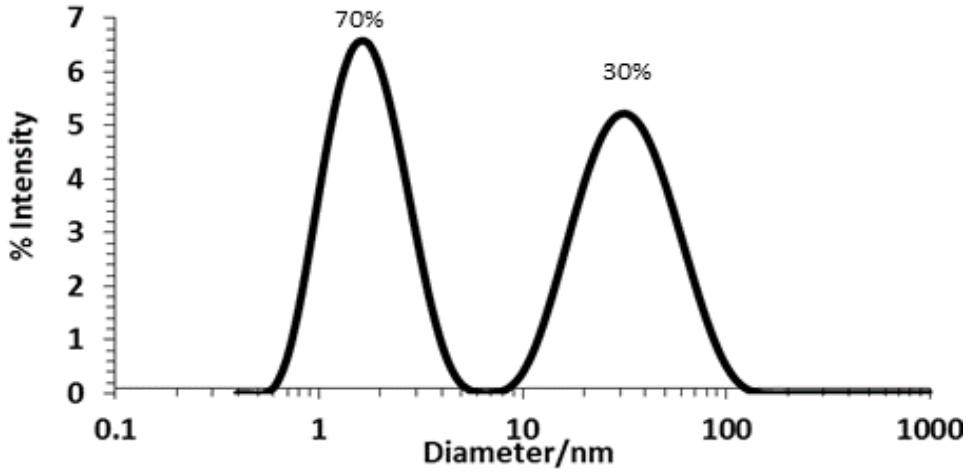



*Figure 7. DLS analysis of pure water AgNPs before dialysis showing particles with a mean diameter of 31.1 nm and a PDI of 0.26. The peak for particles at size 1-10 nm is probably an artefact resulting from impurities or other extraneous scattering sources, while the lower intensity of 30% is for particles of sizes ranging from 10-100 nm.*

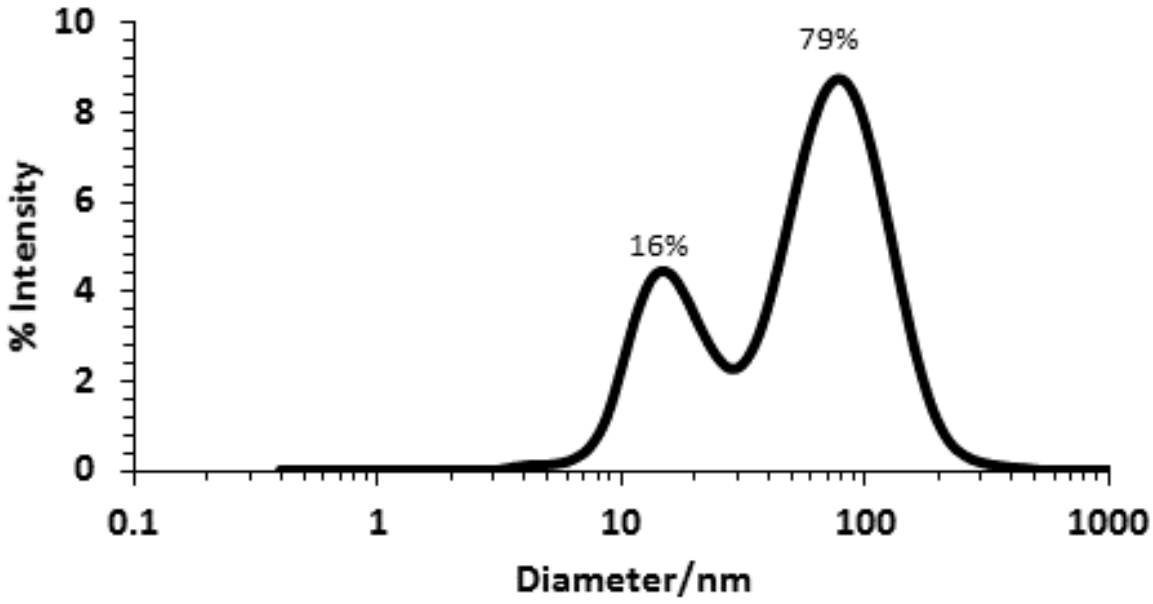


*Figure 8. DLS analysis of pure water AgNPs after dialysis. They are more populated with particles about 100 nm in size with a light scattering intensity of 79%.*

Plots with multiple peaks indicate presence of both isolated and aggregate particles, the latter appearing at longer wavelengths. A clearer picture of this is presented in the analysis histograms of Figure 9 and Figure 10 for pure water AgNPs before and after dialysis, respectively. Polydispersity index (PdI) was evaluated using the equation (2).

$$PDI = \left(\frac{\delta}{d}\right)^2 \qquad (2)$$

where $\delta$ and d stand for standard deviation and mean diameter, respectively.

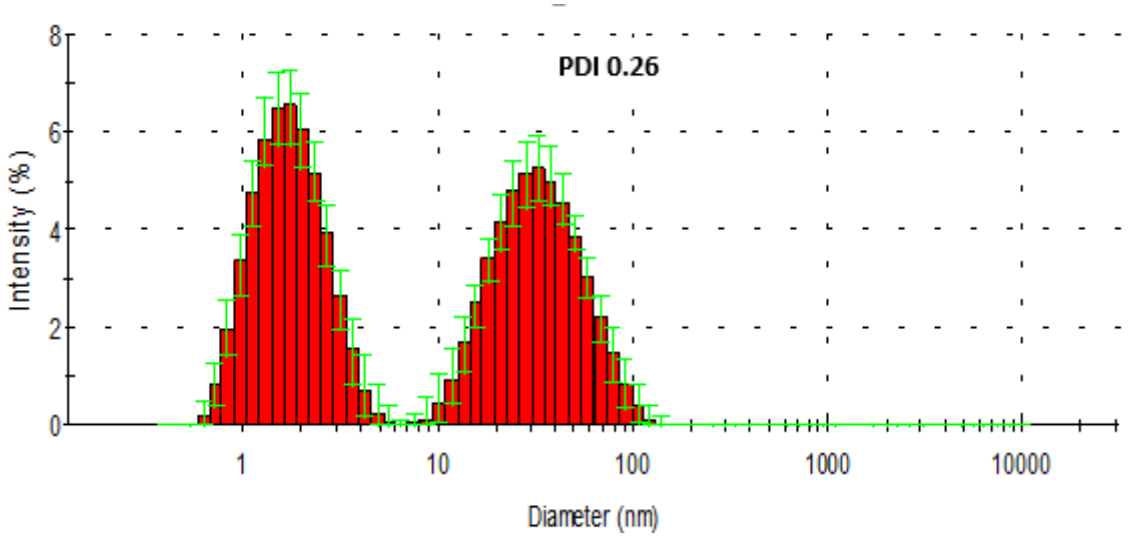



*Figure 9. DLS analysis histogram of pure water AgNPs before dialysis showing the size ranges of the isolated and aggregate particles.*

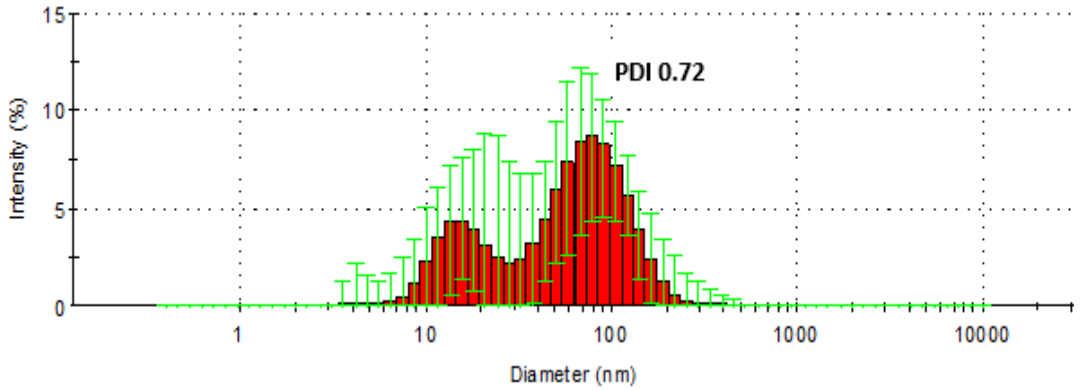



*Figure 10. DLS analysis histogram of pure water AgNPs after dialysis with a PDI value of 0.72 indicating that the particles are highly polydisperse.*

The increase in particle sizes in NaCl-AgNPs is more pronounced than what has been observed in pure water silver nanoparticles, the effect being due to the added ligand and this increases with concentration. Data for the silver nanoparticles infused with 10 mmol NaCl are presented in Figure 11 and Figure 12.

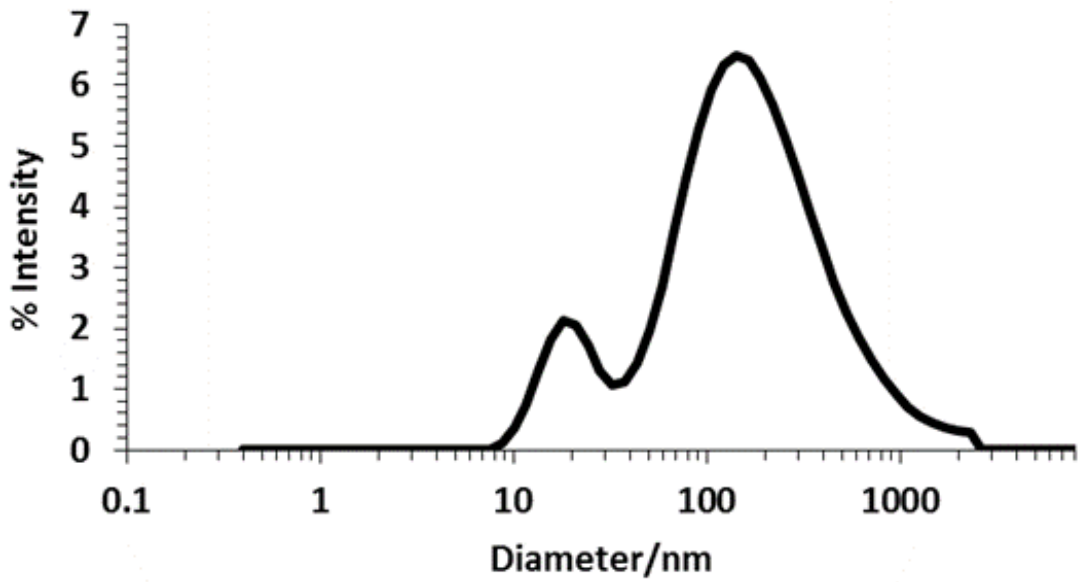



*Figure 11. DLS analysis of 10 mmol NaCl-AgNPs particles before dialysis with diameter of 102 nm and polydispersity index of 0.50.*

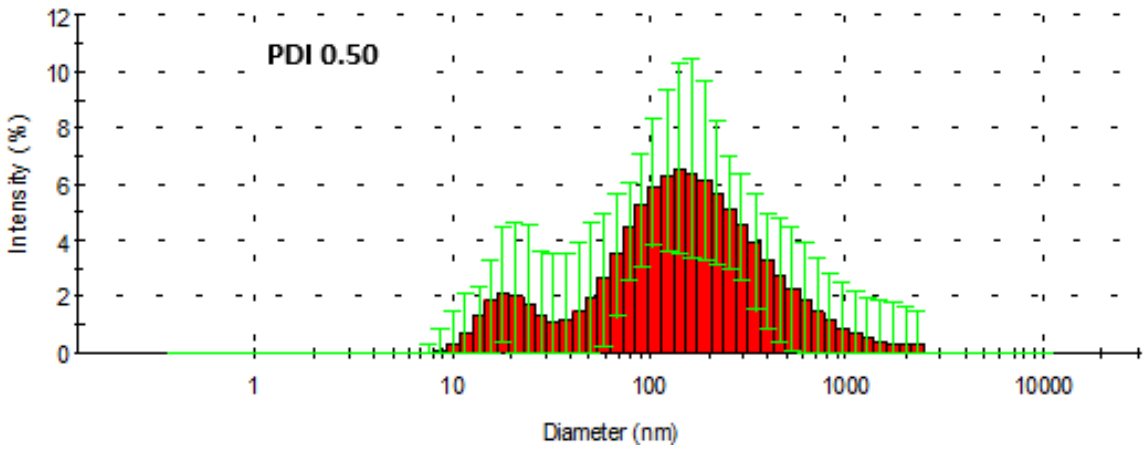



*Figure.12. DLS analysis histogram of 10 mmol NaCl-AgNPs before dialysis*

*From the figures, it's clearly evident that particles of size 100 nm and above are in excess in the NaCl-AgNPs.* A summary of the size measurement data from DLS is presented in Table 1

**Table 1.** Summary of DLS data on particle sizes for pure water and NaCl-AgNPs

| | Pure water | | 10 mmol NaCl | | 30 mmol NaCl | | 50 mmol NaCl | |
|---|---|---|---|---|---|---|---|---|
| | Before dialysis | After dialysis | Before dialysis | After dialysis | Before dialysis | After dialysis | Before dialysis | After dialysis |
| Mean diameter/nm | 31.1 | 34.2 | 102 | 538 | 735 | 990 | 658 | 893 |
| PDI | 0.26 | 0.72 | 0.50 | 0.26 | 0.68 | 0.83 | 0.59 | 0.83 |

From Table (1), it can be observed that there is a general increase in polydispersity index with increasing concentration of NaCl as well as aggregate sizes, and this trend has been reported elsewhere (Pletikapic et al., 2012) with sizes of up to 700 nm. The data, especially size distributions, strongly suggest that the presence of aggregates is responsible for the apparent increase in mean particle diameter with dialysis.

It is to be noted that, where applicable, the AgNPs were not washed prior to dialysis as cleaning would give a false picture of the concentration of Ag(I) released from the preparation into the environment. The dialysis process itself removes the free Ag+ remaining after the preparation. A simple wash would not suffice. It is also worth noting that Ag(I) is continually released by the AgNPs and therefore the dialysis process must be carried out continuously and the dialysate monitored for the Ag(I).

As earlier stated, AFM imaging was done in the tapping mode and the images obtained, therefrom, were processed and analysed using Nanoscope ™ software version 1.4. Apart from the standard flattening of the raw images in software to remove artefacts related to drift, all the images are presented as acquired. The sizes of particles in terms of both height and diameter were observed to decrease after dialysis for both 10 mmolol and 50 mmol NaCl-AgNPs. Sample AFM images of the 10 mmol concentration of AgNPs before and after dialysis, together with their grayscales and some line profiles are shown in Figure 13. The rest of the data on particle sizes of NaCl-AgNPs are summarized in Table 2.

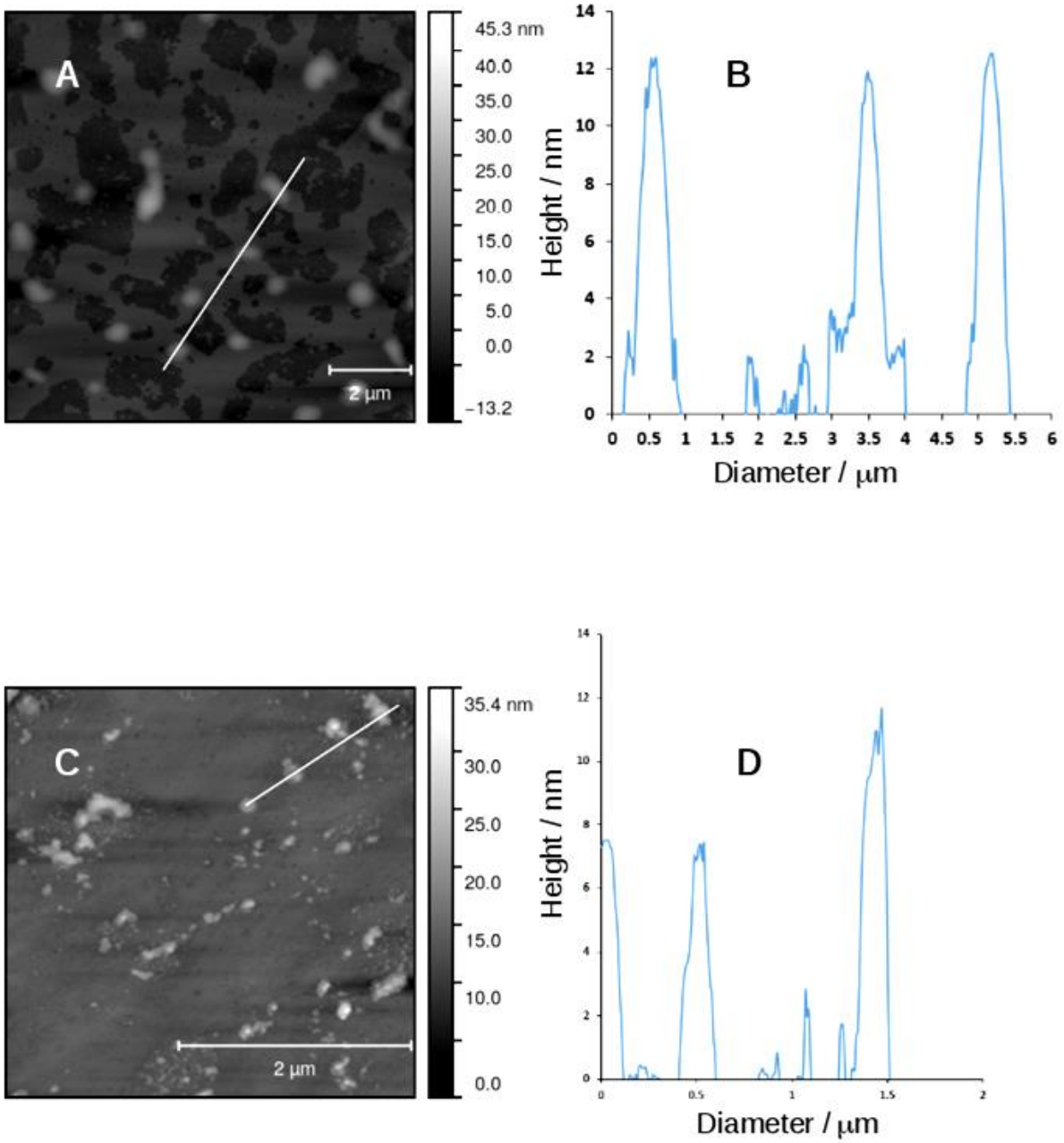



*Figure 13. (A) AFM image of 10 mmol NaCl-AgNps before dialysis (B) the line profile of 03 particles along the white line in A (C) 10 mmol NaCl-AgNPs after dialysis and (D) a line profile along the white line in (C).The scale bars are as indicated on the images. The sample aliquot was drop cast on Si wafer that had been cleaned with acidic piranha solution, thoroughly rinsed with nanopure water and dried with a stream of nitrogen gas.*

**Table 2.** Summary of AFM data obtained for NaCl-AgNPs. SD is the standard deviation of the feature height (Ht) or of the feature lateral diameter (dia) in nm.

| Concentration/mM | | Image no. | Total count | Mean height/nm | SD (Ht) | Mean diameter/nm | SD (Dia) | Scan size/µm |
|---|---|---|---|---|---|---|---|---|
| 10 | Before dialysis | 0.001 | 19 | 104 | 76.5 | 451 | 385 | 10 for all |
| | | 0.002 | 53 | 80.4 | 57.8 | 283 | 193 | |
| | | 0.003 | 21 | 15.4 | 9.00 | 553 | 199 | |
| | | 0.004 | 81 | 54.6 | 21.9 | 334 | 195 | |
| | After dialysis | 0.001 | 126 | 17.1 | 12.9 | 199 | 102 | 10.0 |
| | | 0.002 | 96 | 7.83 | 3.73 | 85.9 | 56.6 | 3.50 |
| | | 0.004 | 55 | 27.7 | 31.4 | 210 | 134 | 10.8 |
| | | 0.013 | 56 | 11.3 | 4.93 | 67.5 | 21.9 | 3.0 |
| | | 0.014 | 53 | 12.6 | 3.19 | 71.3 | 17.4 | 3.3 |
| 30 | Before dialysis | 0.001 | 43 | 10.9 | 2.70 | 49.8 | 8.91 | 4.0 |
| | | 0.002 | 44 | 4.08 | 2.44 | 24.7 | 12.9 | 1.0 |
| | | 0.003 | 93 | 8.81 | 0.84 | 48.4 | 4.23 | 4.0 |
| | | 0.004 | 62 | 8.64 | 0.85 | 47.2 | 3.33 | 4.0 |
| | After dialysis | 0.003 | 12 | 14.3 | 3.91 | 143 | 56.0 | 10.0 |
| | | 0.004 | 9 | 135 | 81.7 | 290 | 205 | 5.0 |
| | | 0.004(a) | 15 | 21.0 | 14.5 | 112 | 70.5 | 4.0 |
| | | 0.005(a) | 13 | 12.6 | 9.23 | 90.1 | 48.9 | 4.5 |
| 50 | Before dialysis | 0.001 | 33 | 13.9 | 3.50 | 89.1 | 16.4 | 4.0 for all |
| | | 0.002 | 28 | 14.8 | 3.67 | 77.9 | 18.1 | |
| | | 0.003 | 33 | 15.3 | 1.87 | 89.8 | 10.7 | |
| | | 0.005 | 16 | 13.6 | 7.43 | 77.81 | 28.6 | |
| | After dialysis | 0.001 | 6 | 9.82 | 3.28 | 78.8 | 13.8 | 4.0 for all |
| | | 0.002 | 17 | 8.48 | 1.75 | 74.2 | 33.3 | |
| | | 0.003 | 30 | 8.71 | 2.25 | 65.2 | 18.1 | |
| | | 0.004 | 14 | 5.80 | 2.05 | 73.6 | 34.0 | |

Sample diameter histograms of the 10 mmol NaCl-AgNPs are also presented in Figure 14 to give a clearer picture of the size distributions of the particles before and after dialysis.

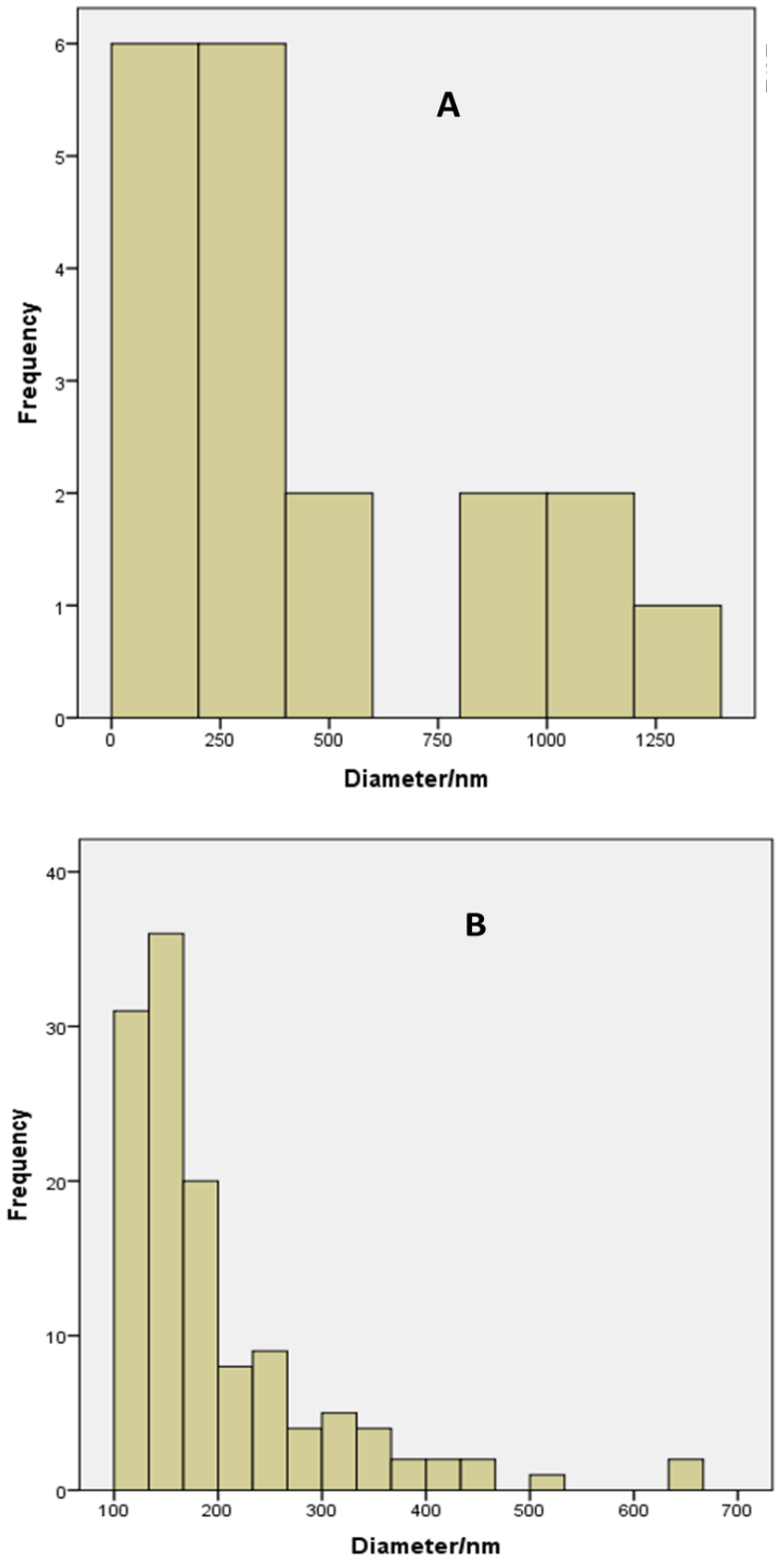



*Figure 14. (A) Diameter histogram of 10 mmol NaCl(aq)-AgNPs before dialysis showing 19 particles with a mean size of 451 nm and standard deviation of 385 nm. (B) Diameter histogram of 10 mmol NaCl(aq)-AgNPs after dialysis showing 126 particles with a mean size of 199 nm and standard deviation of 102 nm.*

The decrease in size is consistent with corrosion of the AgNPs. In spite of aggregation, nanoislands about 1 particle in height deposit on the AFM substrate of silicon wafer. The tip, therefore, recognizes

the height of these islands as, on average, that of single particles.

The $Na_2SO_4$(aq)-AgNPs also showed a general decrease in size, both in terms of height and diameter as was the case with NaCl(aq)-AgNPs. The particles of $Na_2SO_4$(aq)-AgNPs are however much larger than those of the NaCl(aq)-AgNPs. This could be due to adsorption of sulphate ions on the surface of the AgNPs. The solubility product value of 1.4 x $10^{-5}$ at 25 $^oC$ as well as a standard reduction potential of 0.653 V for $Ag_2SO_4$ suggests that the Ag(I) ions have relatively low affinity for sulphate ions. This partly explains why a high concentration of $Ag^+$ ions were released upon dialysis of the $Na_2SO_4$(aq)-AgNPs. The solubility product of AgCl is 1.8 X $10^{-10}$ at 25 $^oC$ and with a relatively low electrode potential for Ag/AgCl of 0.222 V, the interaction between $Ag^+$ and $Cl^-$ is much stronger.

Sample AFM images of the $Na_2SO_4$(aq)-AgNPs are shown in Figure 15

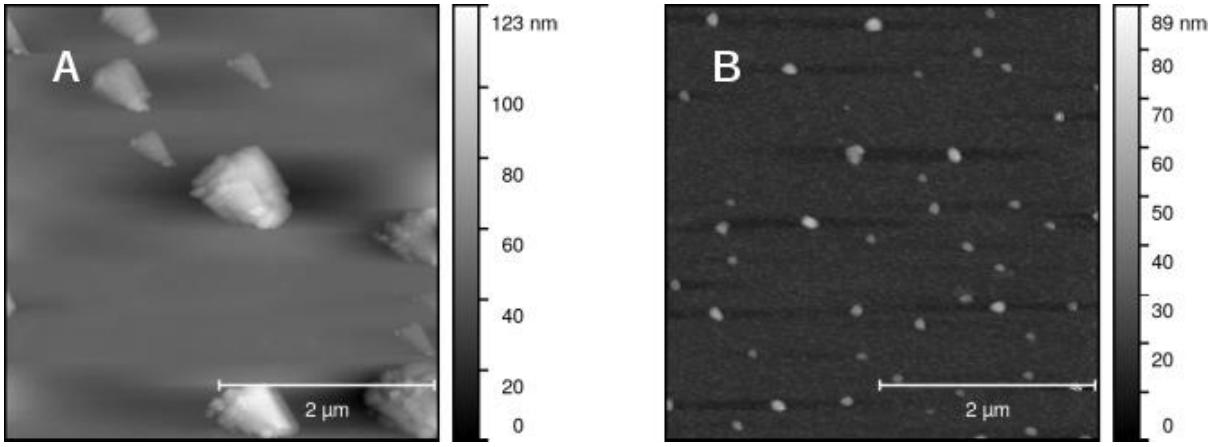



*Figure 15. AFM images of 10 mmol $Na_2SO_4$(aq)-AgNPs (A) before dialysis and (B) after dialysis; all with scan size of 4 µmol and scale bars as indicated on the images. The sample aliquot was drop cast on Si wafer that had been cleaned with acidic piranha solution, thoroughly rinsed with nanopure water and dried with a stream of nitrogen gas.*

Diameter histograms of the 10 mmol $Na_2SO_4$(aq)-AgNPs are also presented in Figure 16 to show the size distribution of the particles more clearly.

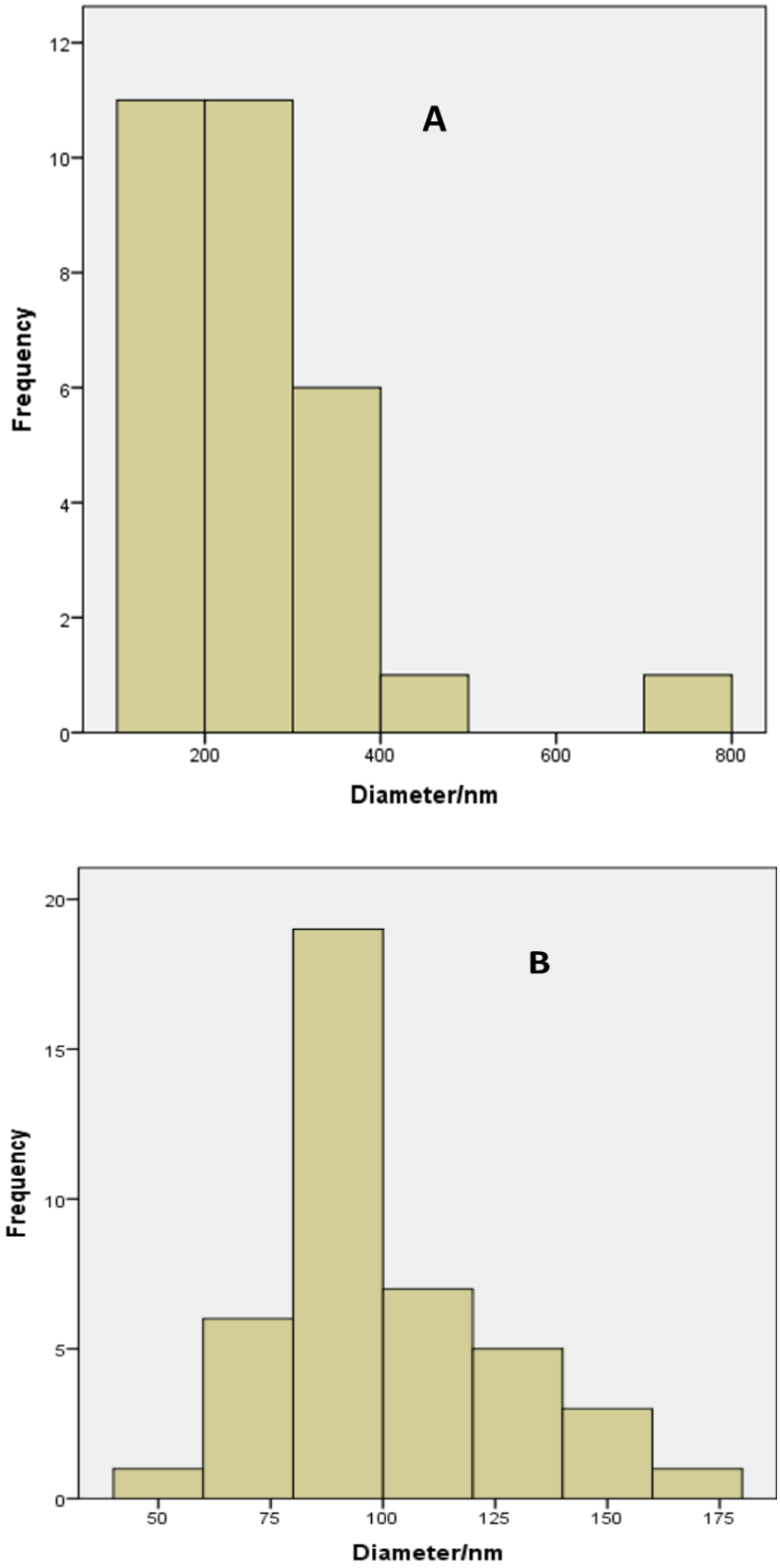



*Figure 16. (A) Diameter histogram of 10 mmol $Na_2SO_4$(aq)-AgNPs before dialysis showing 30 particles with a mean size of 254 nm and a standard deviation of 121 nm. (B) Diameter histogram of 10 mmol $Na_2SO_4$(aq)-AgNPs after dialysis showing 42 particles with a mean size of 100 nm and a standard deviation of 25.1 nm.*

It is to be observed that, in all cases of NaCl(aq)- and $Na_2SO_4$(aq)-AgNPs, the lateral diameters of the particles are larger than their heights. Although small differences between diameter and height could be attributed to tip dilation which brings about an extended diameter size (Alahmad, 2014, Alahmad et al., 2013; Klapetek et al., 2012; Wong et al., 2007), the effects here are large and best understood in terms of aggregation of AgNPs on the Si substrates. The height is less influenced by tip or probe effects and related directly to the particle diameter in the case of island formation of AgNPs on the substrate.

The amount of Ag(I) ions released from the nanoparticles through the dialysis membrane was monitored by stripping voltammoletry at glassy carbon, with $Hg/Hg_2SO_4$ as reference electrode for an accumulation time of 30 s. The accumulation time was increased to 300 s for dialysate fractions in which a stripping curve was not observable after 30 s of pre-concentration time. In such cases, the signal was scaled by a factor of 10 to take account of the change in deposition time. Samples of stripping curves have been presented in Figure 3 above, while an example of baseline corrected data from integration of such curves is as shown in Figure 17.

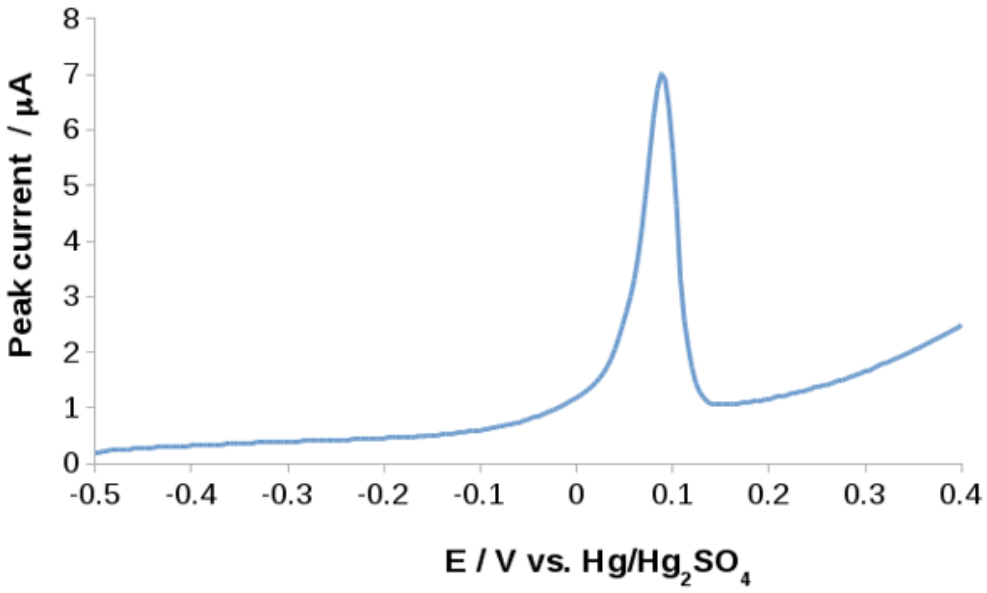



*Figure 17. Anodic stripping voltammogram for 20 µmol $AgNO_3$(aq) in 0.1 mol $NaNO_3$(aq). The data is presented as was acquired, after baseline correction. The Ag stripping peak is observed just below 0.1 V and the scan rate was 1 V $s^{-1}$.*

Values of Ag(I) ion concentration were obtained using the baseline corrected calibration equation 3 obtained by standard addition measurements using $AgNO_3$(aq) standards.

$$Q_p = 0.00106[Ag(I)] - 0.00355 \quad (R^2 = 0.946) \qquad (3)$$

$Q_p$ is the integral of the stripping peak in µC and [Ag(I)] is the Ag(I) concentration in µmol, the calibration curve is not shown. Results of the plots using equation (3) showed a substantial amount of 90 µmol Ag(I) ions present in the initial nanoparticle preparation in the absence of any deliberately added electrolyte. After 73 h of dialysis, about 4 µmol of Ag(I) ions could be detected. Almost the same

concentration of Ag(I) was observed in experiments with deliberately added NaCl(aq), irrespective of the concentration of chloride ions present. The concentration of Ag(I) ions in the dialysate from the experiments with pure water and NaCl(aq)-AgNPs is presented in Figure 18.

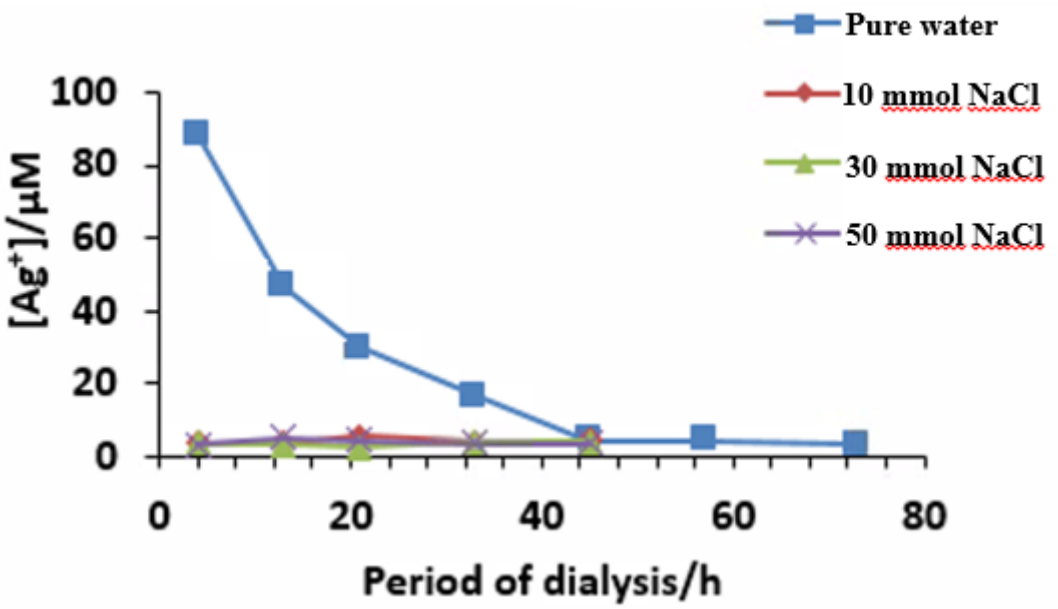



*Figure 18. Variation of [Ag(I)] with time of dialysis for four different sets of experiments to show the composition of the medium against which the sample was dialysed.*

Anodic stripping voltammetry has been used elsewhere to quantify Ag in NPs (Cloake et al., 2015). Complications in the analysis due to aggregation of the AgNPs and effects of the capping ligand were reported. In this work, a different approach and aimed to measure the free Ag(I) in solution produced by corrosion of AgNPs was taken under ambient conditions in various aqueous electrolytes. To avoid issues related to oxidation of AgNPs and unreacted material (citrate) a dialysis technique was employed in which the dialysate was analysed by anodic stripping voltammetry. The concentration of dissolved Ag(I) is of the same order in the presence or absence of chloride. In fact, the data show that at long durations, the concentrations of Ag(I) released are of the order of µmol even in 50 mmol NaCl(aq). This finding is important in the study to the fate of AgNPs in marine environments.

## CONCLUSIONS

From the findings of this work, the following conclusions can be made: The surface plasmon resonance (SPR) of the AgNP sols was blue-shifted for pure water–AgNPs, suggesting corrosion and reduction in particle size. The SPR peak for $Na_2SO_4$ – AgNPs was red-shifted suggesting aggregation.

Taken together, AFM and DLS data show that the AgNPs aggregate during dialysis and that the mean particle size appears to increase because of this. However, a more detailed analysis of the DLS and AFM data shows that the size of individual nanoparticles generally decreased with time of dialysis.

The dialysis experiment showed the steady release of micromolar [Ag(I)] in the presence of up to 50 mmol NaCl(aq) because of corrosion of the AgNPs. The concentration of chloride in a water sample has little influence on the release of Ag(I)

from AgNPs. Presence of sulphates does not exert significant influence on the release of Ag(I) ions from a product or substrate.

**Acknowledgements**

A. S. Nomor appreciates Rev. Fr. Moses Orshio Adasu University, (formerly Benue State University) Makurdi and the Nigerian Tertiary Education Trust Fund (TETFUND) for funding, as well as University Newcastle upon Tyne, UK for providing the facilities.

**Conflict of Interests**: None.

## REFERENCES

Aghari, S., Johari, S. A., Lee, J. H., Kim, Y. S., Jeon, Y. B., Choi, H. J., Moon, M. C. &Yu, I. J. (2012). Toxicity of various silver nanoparticles compared to silver ions in *Daphnia magna*. *Journal of Nanobiotechnology 10*, 1-11

Alahmad, A. (2014). Preparation and Characterization of Silver Nanoparticles. *Internation Journal of ChemTech Research 6*, 450-459

Alahmad, A., Eleoui, M., Falah, A. & Alghorabi, I. (2013). Praparation of colloidal silver nanoparticles and structural characterization. *Physical Sciences Research International 1*, 89-96

Benn, M.T. & Westerhoff, P. (2008). Nanoparticle Silver Released into Water from Commolercially Available Sock Fabrics. *Environ. Sci. Technol. 42*, 4133-4139

Bratsch, S.G. (1989) Standard Electrode Potentials and Temperature Coefficients in Water at 298.15 K. *Journal of Physical Chemistry Reference Data 18*, 1-21

Cloake, S.J., Toh, H. S., Lee, P. T., Salter, C., Johnston, C. & Compton, R. G. (2015). Anodic stripping voltammoletry of silver nanoparticles: aggregation leads to incomplete stripping. *ChemistryOpen 4*, 22-26

Dankovich, T.A. & Gray, D.G. (2011). Bactericidal paper impregnated with silver nanoparticles for point-of-use water treatment. *Environ Sci Technol 45*, 1992-1998

Espinoza, M.G., Hinks, M.L., Mendoza, A.M., Pullman, D.P. & Peterson, K.I. (2012). Kinetics of Halide-Induced Decomposition and Aggregation of Silver Nanoparticles. *The Journal of Physical Chemistry C 116*, 8305-8313

Geranio, L., Heuberger, M. & Nowack, B. (2009) The Behaviour of silver nanotextiles during washing. *Environ. Sci. Technol. 43*, 8113-8118

Ghosh, S.K. & Pal, T. (2007). Interparticle Coupling Effect on the Surface Plasmon Resonance of Gold Nanoparticles: From Theory to Applications. *Chemical Reviews 107*, 4797-4862

Hebeish, A., El-Rafie, M.H., El-Sheikh, M.A., Seleem, A.A. & El-Naggar, M.E. (2014). Antimicrobial wound dressing and anti-inflammolatory efficacy of silver nanoparticles. *Int J Biol Macromol 65*, 509-515

Hu, L., Hu, S., Guo, L., Tang, T. & Yang, M. (2016). Optical and electrochemical detection of biothiols based on aggregation of silver nanoparticles. *Analytical Methods 8*, 4903-4907

Ijaz-Hussain, J., Kumar, S., Adil-Hashmi, A. & Khan, Z. (2011). Silver Nanoparticles: Preparation, Characterization and Kinetics. *Advanced Materials Letters 2*, 188-194

Kaegi, R., Voegelin, A., Sinnet, B., Zuleeg, S., Hagendorfer, H., Burkhardt, M. & Siegrist, H. (2011). Behavior of metallic silver nanoparticles in a

pilot wastewater treatment plant. *Environ Sci Technol 45*, 3902-3908

Khan, Z., Hussain, J.I., Kumar, S., Hashmi, A.A. & Malik, M.A. (2011). Silver Nanoparticles: Green Route, Stability and Effect of Additives. *Journal of Biomaterials and Nanobiotechnology 02*, 390-399

Klapetek, P., Valtr, M., Necas, D., Salyk, O. & Dzik, P. (2011). Atomic force microscopy analysis of nanoparticles in non-ideal conditions. *Nanoscale Research Letters* ***6***, 1-9

Kuyper, A.C. (1933). The Oxidation of Citric Acid. *J. Am. Chem. Soc. 55*, 1722-1727

Lee, P.C. & Meisel, D. (1982). Adsorption and surface-enhanced Raman of dyes on silver and gold sols. *Journal of Physical Chemistry 86*, 3391-3395

Maneerung, T., Tokura, S. & Rujiravanit, R. (2008) Impregnation of silver nanoparticles into bacterial cellulose for antimicrobial wound dressing. *Carbohydrate Polymers 72*, 43-51.

Meyer, D.E., Curran, M.A. & Gonzalez, M.A. (2010) An examination of silver nanoparticles in socks using screening-level life cycle assessment. *Journal of Nanoparticle Research 13*, 147-156

Nanda, A. & Saravanan, M. (2009). Biosynthesis of silver nanoparticles from *staphylococcus aureus* and its ANTImicrobial activity against MRSA and MRSE. *Nanomedicine: Nanotechnology, Biology, and Medicine 5*, 452-456

Odzak, N., Kistler, D., Behra, R. & Sigg, L. (2014). Dissolution of metal and metal oxide nanoparticles in aqueous media. *Environmental Pollution 191*, 132-138

Pletikapic, G., Zutic, V., Vrcek, I.V. & Svetlicic, V. (2012). Atomic force microscopy characterization of silver nanoparticles interactions with marine diatom cells and extracellular polymeric substance. *Journal of Molecular Recognition 25*, 309-317

Sharma, V.K., Yngard, R.A. & Lin, Y. (2009). Silver nanoparticles: green synthesis and their antimicrobial activities. *Adv Colloid Interface Sci 145*, 83-96

Shrivas, K., Sahu, S., Patra, G.K., Jaiswal, N.K. & Shankar, R. (2016). Localized surface plasmon resonance of silver nanoparticles for selective colorimetric detection of chromium in surface water, industrial waste water and vegetable samples. *Analytical Methods 8*, 2088-2096

Sohn, E.K., Johari, S. A., Kim, T. G., Kim, J. K., Kim, E., Lee, J. H., Chung, Y. S & Yu, I. J. (2015). Aquatic Toxicity Comparison of Silver Nanoparticles and Silver Nanowires. *Biomed Res Int 2015*, 893049

Solomon, S.D., Bahadory, M., Jeyarajasingam, A.V., Rutkowsky, S.A. & Boritz, C. (2007). Synthesis and study of silver nanoparticles. *Journal of Chemical Education 84*, 322-325

Suchomel, P., Kvitek, L., Panacek, A., Prucek, R, Hrbac, J., Vecerova, R. & Zboril, R. (2015) Comparative study of antimicrobial activity of AgBr and Ag nanoparticles (NPs). *Plos One*, 1-15

Toh, H.S., Jurkschat, K. & Compton, R.G. (2015). The Influence of the Capping Agent on the Oxidation of Silver Nanoparticles: Nano-impacts versus Stripping Voltammoletry. *Chemistry A European Journal*, 2998-3004

Udapudi, B., Naik, P., Savadatti, S.T., Sharma, R. & Balgi, S. (2012). Synthesis and characterization of silver nanoparticles. *International Journal of Pharmacy and Biological Sciences 2*, 10-14

Wang, H., Qiao, X., Chen, J. & Ding, S. (2005). Preparation of silver nanoparticles by chemical reduction method. *Colloids and Surfaces A: Physiochem. Eng. Aspects 256*, 111-115

Wilkinson, L.J., White, R.J. & Chipman, J.K. (2011). Silver and nanoparticles of silver in wound dressings: a review of efficacy and safety. *J Wound Care 20*, 543-549

Wong, C., West, P.E., Oslon, K.S., Mecartney, M.L. & Starostina, N. (2007). Tip dilation and AFM capabilities in the characterization of nanoparticles. *JOM: Journal of Minerals, Metals and Materials Society 59*, 12-16

World Health Organization. (2003). Silver in drinking-water. Background document for development of WHO guidelines for drinking- water quality, Vol. 2, 2nd ed. (WHO, Geneva,).